Silencing SPP1 in M2 macrophages inhibits the progression of castration-resistant prostate cancer via the MMP9/TGFβ1 axis

Saipeng Chen[1#], Bingqian Deng[2#], Fuhan Zhao[1#], Hang You[3], Youxin Liu[1], Langlang Xie[2], Guojing Song[1], Zhansong Zhou[1], Gang Huang[2^], Wenhao Shen[1]

[1]Department of Urology, Southwest Hospital, Army Medical University (Third Military Medical University), Chongqing, China; [2]Department of Biochemistry and Molecular Biology, College of Basic Medical Science, Army Medical University (Third Military Medical University), Chongqing, China; [3]Key Laboratory of Molecular Biology for Infectious Diseases (Ministry of Education), Institute for Viral Hepatitis, Department of Infectious Diseases, The Second Affiliated Hospital, Chongqing Medical University, Chongqing, China

Contributions: (I) Conception and design: S Chen; (II) Administrative support: Z Zhou; (III) Provision of study materials or patients: Z Zhou, W Shen; (IV) Collection and assembly of data: S Chen, B Deng, F Zhao, G Song, Y Liu, L Xie; (V) Data analysis and interpretation: S Chen; (VI) Manuscript writing: All authors; (VII) Final approval of manuscript: All authors.

[#]These authors contributed equally to this work.

Correspondence to: Wenhao Shen, PhD. Department of Urology, Southwest Hospital, Army Medical University (Third Military Medical University), 30 Gaotan Yanzheng Street, Shapingba District, Chongqing 400038, China. Email: chongqingswh@aliyun.com; Gang Huang, PhD. Department of Biochemistry and Molecular Biology, College of Basic Medical Science, Army Medical University (Third Military Medical University), 30 Gaotan Yanzheng Street, Shapingba District, Chongqing 400038, China. Email: cqhuanggang@aliyun.com; Zhansong Zhou, PhD. Department of Urology, Southwest Hospital, Army Medical University (Third Military Medical University), 30 Gaotan Yanzheng Street, Shapingba District, Chongqing 400038, China. Email: zzs68754186@163.com.

Background: M2 macrophages can promote the progression of castration-resistant prostate cancer (CRPC), but the specific mechanism is still unclear. Therefore, we are preliminarily exploring the molecular mechanism by which M2 macrophages regulate the progression of CRPC.

Methods: The genes positively correlated with CRPC and with the most significant differences in the GEO32269 dataset were obtained. Database and immunofluorescence experiments were used to validate the localization of secreted phosphoprotein 1 (SPP1) in localized prostate cancer (PCa), hormone-sensitive prostate cancer (HSPC), and CRPC tumor tissues. The function of SPP1 in M2 macrophages was verified through cell scratch, Transwell, and an orthotopic PCa model. PCa database and Western blot were used to verify the relationship between SPP1 and matrix metallopeptidase 9 (MMP9), as well as the ability of MMP9 in M2 macrophages to promote epithelial-mesenchymal transition (EMT) in PCa cells.

Results: The primary localization of SPP1 in prostate and CRPC tissues is in macrophages. Silencing SPP1 expression in M2 macrophages promotes their polarization towards the M1 phenotype and significantly inhibits the malignant progression of PCa *in vitro* and *in vivo*. SPP1 promotes the expression of MMP9 through the PI3K/AKT signaling pathway in M2 macrophages. Furthermore, MMP9 enhances the EMT and migratory capabilities of PC3 cells by activating the TGFβ signaling pathway.

Conclusions: We have found that the high expression of SPP1 in M2 macrophages promotes the progression of CRPC through cell-cell interactions. These findings can contribute to the development of novel therapeutic approaches for combating this deadly disease.

Keywords: Castration-resistant prostate cancer (CRPC); secreted phosphoprotein 1 (SPP1); matrix metallopeptidase 9 (MMP9); transforming growth factor beta signaling pathway (TGFβ signaling pathway); epithelial-mesenchymal transition (EMT)

^ ORCID: 0000-0001-6850-940X.

Introduction

Prostate cancer (PCa) is a common malignant tumor of the urinary system in men, and its incidence and mortality rates have been steadily increasing in Western countries [1]. Following prolonged androgen deprivation therapy (ADT), the majority of PCa patients inevitably progress to castration-resistant prostate cancer (CRPC) [2]. Recent research has found that in CRPC patients with bone metastasis, M2 macrophages are the main cellular population in the tumor microenvironment (TME), indicating that tumor-associated macrophages (TAMs) may play a crucial role in mediating the progression of CRPC [3]. However, the specific mechanisms by which macrophages influence the progression of PCa remain unclear.

TME forms the foundation for tumor metastasis with its complex cellular components. Cell populations commonly found within this microenvironment, such as fibroblasts and macrophages, play a crucial role in tumor progression [4,5]. Targeted therapies focusing on relevant cells within the TME have shown promise in inhibiting tumor progression [6,7]. PCa is known for its cold immune response to immunotherapy. The main reason is that the relevant immune cells are unable to heavily infiltrate the TME of PCa [8]. Nevertheless, recent research has revealed a high abundance of macrophages in CRPC tissues [3]. In addition, a high abundance of macrophages can suppress T cell activity, leading to an immunosuppressive microenvironment that promotes castration-resistant progression of PCa [9]. Thus, targeting macrophages has emerged as a potential approach for PCa treatment [10].

One important molecule of interest is secreted phosphoprotein 1 (SPP1), also known as osteopontin, which is a multifunctional secreted phosphorylated glycoprotein [11]. SPP1 is primarily expressed in bone-forming cells, fibroblasts, macrophages, dendritic cells, lymphocytes, and monocytes within the immune system [12]. Research has demonstrated a high expression of SPP1 in solid organ tumors [13]. Furthermore, SPP1 is also considered a biomarker of M2 macrophages, and recent research indicates that the ratio of CXCL9/SPP1 expression in macrophages can serve as a marker for measuring macrophage polarization [11,14]. SPP1 in macrophages has been shown to promote tumor metastasis and malignant progression in various types of cancer [14-17]. Ramadan *et al.* found that continuous oral administration of 100 mg/kg thioacetamide (TAA) significantly inhibited the expression of SPP1 in liver fibrosis tissues [18]. However, the potential of SPP1 to promote tumor metastasis within macrophages has not yet been explored in PCa research.

In our study, analysis of the GSE32269 dataset revealed that SPP1 exhibited the highest differential expression in metastatic CRPC (mCRPC) tissues compared to localized PCa. Additionally, we found that SPP1 is mainly expressed in mononuclear macrophages in the PCa single-cell RNA sequencing (scRNA-seq) database. Through *in vitro* and *in vivo* experiments, it was confirmed that high expression of SPP1 in M2 macrophages promotes PCa metastasis. Mechanistic studies have elucidated a robust correlation between SPP1 and matrix metallopeptidase 9 (MMP9), highlighting that SPP1 regulates the expression of MMP9 in M2 macrophages through the PI3K/AKT signaling pathway. MMP9 is known to activate the extracellular secretion of transforming growth factor beta 1 (TGFβ1) by cleaving TGFβ1 protein [19]. In summary, our study provides evidence that high expression of SPP1

Highlight box

Key findings
- This study proposes that the high expression of secreted phosphoprotein 1 (SPP1) in M2 macrophages can promote epithelial-mesenchymal transition in castration-resistant prostate cancer (CRPC) cells through the matrix metallopeptidase 9 (MMP9)/transforming growth factor beta 1 (TGFβ1) signaling pathway, thereby enhancing the progression of CRPC.

What is known and what is new?
- M2 macrophages play an important role in the progression of CRPC.
- It is still unclear whether the high expression of SPP1 in M2 macrophages is an important factor promoting the progression of CRPC.

What is the implication, and what should change now?
- This research result suggests that targeted therapy for SPP1 has the potential to inhibit the tumor promoting effect of M2 macrophages, thereby inhibiting the progression of prostate cancer.

Table 1 SiRNA sequence

Gene	Sense	Anti-sense
SPP1-1	CCAAAGUCAGCCGUGAAUU	AAUUCACGGCUGACUUUGG
SPP1-2	GUAAGGAAGAAGAUAAACA	UGUUUAUCUUCUUCCUUAC
SPP1-3	GGUCAAAAUCUAAGAAGUU	AACUUCUUAGAUUUUGACC
MMP9	CAAGACAAAGCCUAUUUCUTT	AGAAAUAGGCUUUGUCUUGTT

siRNA, small interfering RNA.

in M2 macrophages is an important factor in promoting PCa metastasis, and SPP1 exerts its effects through the regulation of MMP9/TGFβ1. We present this article in accordance with the MDAR and ARRIVE reporting checklists (available at https://tau.amegroups.com/article/view/10.21037/tau-24-127/rc).

Methods

Bioinformatics analysis

In the Gene Expression Omnibus (GEO) database, we analyzed the transcriptomic sequencing data of GSE32269 and performed a volcano plot analysis. In the PCa database (https://bioinformatics.cruk.cam.ac.uk/apps/camcAPP/), we analyzed the relationship between the expression of SPP1 and the progression of PCa. The UALCAN (https://ualcan.path.uab.edu/index.html) and GEPIA (http://gepia.cancer-pku.cn/index.html) databases were used to analyze the association of SPP1 expression with Gleason score, tumor-node-metastasis (TNM) stage, and patient survival in PCa. The single-cell database TISCH2 (http://tisch.comp-genomics.org/) was utilized to analyze the cell clustering of different types of PCa and the cellular distribution of SPP1. The Timer2 (http://timer.cistrome.org/) and cBioPortal (https://www.cbioportal.org/) databases were employed to analyze the expression of SPP1 in PCa and its relationship with M1/M2 macrophages. The Kyoto Encyclopedia of Genes and Genomes (KEGG) and gene set enrichment analysis (GSEA) enrichment were performed by the OECloud tools at https://cloud.oebiotech.com. The study was conducted in accordance with the Declaration of Helsinki (as revised in 2013).

Cell culture

The human PCa cell lines PC3 and the human monocytic leukemia cell line THP-1, as well as the mouse PCa cell line RM1 were obtained from American Type Culture Collection (ATCC; Manassas, VA, USA). All four cell lines were cultured in high-glucose Dulbecco's modified Eagle medium (DMEM; Gibco, Grand Island, NY, USA) supplemented with 10% fetal bovine serum (FBS; Gibco) and 1% penicillin/streptomycin. However, THP-1 did not require the addition of 1% penicillin/streptomycin. The cells were maintained at 37 ℃ in a humidified atmosphere containing 0.5% CO_2. Before experimentation, all used cell lines were authenticated through short tandem repeat (STR) analysis and were confirmed to be free of mycoplasma contamination.

Cell transfection

Three specific small interfering RNA (siRNA) targeting SPP1 were designed and constructed by Beijing Tsingke Biotech Co., Ltd. THP-1 cells were seeded in a 6-well plate and induced with 100 ng/mL of phorbol myristate acetate (PMA) [MedChemExpress (MCE), Cat#HY-18739; MCE, Monmouth Junction, NJ, USA] to generate M0 macrophages, followed by induction with IL-4 (MCE, Cat#HY-P70445) to generate M2 macrophages. Subsequently, Lipo3000 transfection reagent (Thermo Fisher Scientific, Waltham, MA, USA) was used for siRNA transfection of the cells. The siRNA sequences used are shown in *Table 1*.

Western blot

Cellular proteins were extracted using radioimmunoprecipitation assay (RIPA) lysis buffer and quantified using a bicinchoninic acid (BCA) assay kit according to the manufacturer's protocol. Then, 2 micrograms of protein were loaded onto sodium dodecyl sulfate polyacrylamide gel electrophoresis (SDS-PAGE) gels and separated by electrophoresis. The proteins were then transferred to immune-blot polyvinylidene

Transl Androl Urol 2024;13(7):1239-1255 | https://dx.doi.org/10.21037/tau-24-127

Table 2 Antibody

Antibodies	Company	Catalog No.	Species	Molecular weight (kDa)
SPP1	Proteintech	22952-1-AP	Rabbit	105
MMP9	Proteintech	10375-2-AP	Rabbit	78
AGR1	Proteintech	66129-1-Ig	Mouse	36
TNFα	Proteintech	26405-1-AP	Rabbit	26
CDH1	Proteintech	60335-1-Ig	Mouse	120
CDH2	Proteintech	66219-1-Ig	Mouse	130
Vimentin	Proteintech	60330-1-Ig	Mouse	57
SNAIL	Proteintech	13099-1-AP	Rabbit	33
PI3K	Zenbio	R381065	Rabbit	56
p-PI3K	Zenbio	341468	Rabbit	58
AKT	Zenbio	R23412	Rabbit	54
p-AKT	Zenbio	R381555	Rabbit	54
Smad2/3	Zenbio	382472	Rabbit	52
p-Smad2/3	Zenbio	251795	Rabbit	52
β-actin	Zenbio	T200068-8F10	Mouse	42

SPP1, secreted phosphoprotein 1; MMP9, matrix metallopeptidase 9; TNF, tumor necrosis factor.

fluoride (PVDF) membranes using a semi-dry transfer apparatus (Bio-Rad, Hercules, CA, USA). The membranes were blocked with a protein-free rapid sealing solution (#G2052, Servicebio, Wuhan, China) for 10 minutes at room temperature, followed by overnight incubation at 4 ℃ with primary antibodies. After washing the membranes three times for 15 minutes each with phosphate-buffered saline with Tween 20 (PBST), they were incubated at room temperature for 1 hour with secondary antibodies specific to the species. The membranes were then washed 3 times with PBST for 15 minutes each time. Protein signal detection was performed using the Ultrasensitive ECL Western HRP Substrate (#17047, ZenBio, Shanghai, China) and a Bio-Rad ChemiDoc MP System (170–8280). The relevant information on the antibodies used in the experiment is shown in *Table 2*.

Real-time quantitative polymerase chain reaction (RT-qPCR)

Total RNA was extracted using a TRIzol reagent (Ambion 317908), and the concentration was determined. The RNA was then reverse transcribed into complementary DNA (cDNA) using PrimeScript Reverse Transcriptase (DRR047A, TaKaRa, Beijing, China). For gene expression analysis, SYBR Green Master Mix (A25742, China) from Thermo Fisher Scientific and primers synthesized by Sangon Biotech (Shanghai, China) were used. RT-qPCR was performed on a Bio-Rad CFX Connect Real-Time System. The gene expression levels were determined using the $2^{-\Delta\Delta Ct}$ method.

Construction of luciferase labeled cells

The RM1 mouse PCa cell line was seeded into a 24-well plate until reaching approximately 75% confluency. Then, 10 µL of blank plasmid lentiviral particles provided by Beijing Tsingke Biotech Co., Ltd. were added and mixed well. After 24 hours, the media was replaced and supplemented with puromycin for selection until stable cells carrying the luciferase fluorescent label were obtained.

Orthotopic PCa model and bioluminescence imaging (BLI)

All animal studies carried out in this project strictly followed the regulations of the China Nature Conservation Committee and were approved by the Animal Experiment Welfare and Ethics Committee of the Army Medical

University (No. AMUWEC20232943), in compliance with institutional guidelines for the care and use of animals. A protocol was prepared before the study without registration. A total of eight C57 male mice aged 4–6 weeks were purchased from the Animal Research Institute of the Third Military Medical University, and four were randomly selected and divided into an experimental group and a control group, respectively. The mice were raised in a sterile specific-pathogen-free (SPF) environment, and the feed and water provided were also treated aseptically. RM1-luciferase cells (1×10^5) were resuspended in 10–20 μL phosphate-buffered saline (PBS) and injected into the prostate of the mice using an insulin needle under a microscope after opening the abdominal cavity and exposing the prostate gland. The surgical site was closed with 4-0 silk thread, and antibiotics were added to the drinking water to prevent infection. BLI, stimulated by D-luciferin potassium salt solution (10 μL/g body weight, #ST198, Beyotime, China), was performed post-surgery using the IVIS Spectrum CT system (PerkinElmer, Waltham, MA, USA) provided by the First Affiliated Hospital of the Third Military Medical University. Subsequently, 0.5% sodium carboxymethyl cellulose (CMC Na) and 0.5% CMC-TAA was administered orally at a dose of 100 mg/kg/day for 15 consecutive days. On the last day, the mice were euthanized and prostate tumor tissue was extracted.

Tibial bone metastasis model

A total of eight C57 mice aged 4–6 weeks were randomly divided into an experimental group and a control group at 5–6 weeks of age, with four mice in each group. The mice were anesthetized with isoflurane gas and the left hind limb was disinfected with alcohol. Using an insulin syringe, 1×10^5 of RM1-luciferase cells were drawn up and resuspended in 20 μL PBS. The insulin needle was slowly inserted vertically along the tibial plateau into the bone marrow cavity for injection, followed by disinfection of the injection site. On the third day after injection, live imaging was performed to detect the fluorescence of the tibia and ensure consistent cell injection. Subsequently, 0.5% CMC-Na and 0.5% CMC-TAA was administered orally at a dose of 100 mg/kg/day for 15 consecutive days. On day 33, the mice were euthanized and their tibias collected, which were fixed in 4% paraformaldehyde for at least 24 hours after decalcification. Relevant indicators were evaluated by hematoxylin and eosin (H&E) staining,

immunohistochemical (IHC) staining, and tartrate-resistant acid phosphatase (TRAP) staining.

Immunohistochemistry and immunofluorescence

The paraffin-embedded PCa tumor tissue was sectioned into 5-mm thick slices. Ethylenediamine tetraacetic acid (EDTA) retrieval was performed at a high temperature for 3 minutes, followed by PBS washing and serum blocking for 1 hour. The corresponding primary antibody was added under dark conditions and incubated overnight at 4 ℃. After PBS washing the next day, the secondary antibody was added and incubated at room temperature for 30 minutes. Immunohistochemistry was performed using 3,3'-diaminobenzidine (DAB) chromogen to visualize the staining. Subsequently, the slides were placed in a hematoxylin solution for 1 minute, rinsed with running water, and air-dried before being covered and slipped. The immunofluorescence steps were conducted the same as for immunohistochemistry, with the addition of 4',6-diamidino-2-phenylindole (DAPI) for nuclear staining. Finally, the slides were sealed with a mounting medium containing an anti-fluorescent quencher.

Flow cytometry

After washing the treated cells with PBS, they were resuspended in 200 μL of PBS and incubated with flow cytometry antibodies according to the appropriate proportions. The antibodies included anti-human CD68 antibody (#11-0689-41, Thermo Fisher Scientific, ASA), anti-human CD163 (#17-1639-41, Thermo Fisher Scientific), and anti-human CD86 (#12-0869-41, Thermo Fisher Scientific) antibodies. M0 macrophages were identified as CD68+, M1 macrophages were identified as CD68+CD86+, and M2 macrophages were identified as CD68+CD163+. The experimental detection instrument (BD LSRFortessa™; Becton, Dickinson, and Co., Franklin Lakes, NJ, USA) was provided by the First Affiliated Hospital of the Third Military Medical University.

Statistical analysis

All data presented in this study are representative of at least three independent replicates. Quantitative data were expressed as the mean ± standard deviation and were analyzed using GraphPad Prism 8 software (GraphPad Software, San Diego, CA, USA). Differences between the

two groups were compared using unpaired *t*-tests. A P value <0.05 was considered statistically significant.

Results

Upregulation of SPP1 is positively correlated with the progression of PCa

To investigate the potential mechanisms underlying CRPC metastasis, we analyzed the GSE32269 dataset containing transcriptomic sequencing data from tumor tissues of 21 patients with localized PCa and mCRPC. Our analysis revealed that SPP1 had the highest differential expression in the mCRPC group (*Figure 1A*). IHC analysis of tumor samples collected from patients at different stages of PCa progression indicated that SPP1 expression was lower in localized PCa but increased in CRPC tissues. Moreover, the highest expression of SPP1 was observed in tumor samples from mCRPC patients (*Figure 1B*). Additionally, the Michigan 2005 and 2012 databases showed higher expression levels of SPP1 in tumor samples from patients with mCRPC than in benign and localized PCa (*Figure 1C*). Analysis of The Cancer Genome Atlas (TCGA) database further revealed a positive correlation between SPP1 expression and the Gleason score, as well as TNM analysis in clinical PCa patients (*Figure 1D,1E*). Furthermore, we observed that patients with high expression of SPP1 had significantly shorter overall survival in the Memorial Sloan Kettering Cancer Center (MSKCC) and TCGA-PRAD (prostate adenocarcinoma) sequencing data (*Figure 1F,1G*). These findings suggest that the high expression of SPP1 in PCa tissue is associated with the malignant progression of PCa.

SPP1 is predominantly expressed in macrophages in PCa tissues

Based on our analysis of the GSE32269 dataset through transcriptomic sequencing, we observed a significantly high expression of SPP1 in mCRPC tumor tissues, indicating a substantial differential fold change. However, due to the intricate cellular composition within the TME, it remained challenging to identify the predominant cell type responsible for SPP1 expression. To address this, we initially examined the Human Protein Atlas (HPA) database to analyze the cellular components associated with SPP1. Interestingly, our findings revealed a strong correlation between SPP1 and macrophage markers (C1QA, LRRC25,

VSIG4) in the prostate (*Figure 2A,2B*). Moreover, when investigating three PCa single-cell datasets (GSE137829, GSE141445, GSE176031) in the TISHC2 tumor single-cell database, we discovered that SPP1 is primarily expressed in monocyte-derived macrophages, whereas its expression in other cell types is minimal (*Figure 2C,2D*). Additionally, immunofluorescence staining performed on tumor tissues from clinical PCa patients exhibited co-localization of SPP1 and CD206 in mCRPC tumor tissues (*Figure 2E*). Taken together, these findings suggest that SPP1 is primarily expressed in M2 macrophages within PCa.

The plasticity regulation of macrophage polarization is mediated by the expression of SPP1

Macrophages are a prominent component of the complex PCa microenvironment. To explore the relationship between SPP1 and macrophage polarization, we analyzed the correlation between SPP1 and M1/M2 macrophage polarization markers in the SU2C-mCRPC dataset. Our findings revealed a significantly higher correlation between SPP1 and M2 macrophage markers (CD206, CD115, CD163, IL-10, CXCL3, CCL18) compared to M1 markers (TNFα, NOS2, CXCL10, CD86, CD80) (*Figure 3A,3B*). Moreover, analysis of the PCa immune infiltration database indicated that high SPP1 expression is more strongly associated with M2 macrophage infiltration than with M1 and M0 macrophages (*Figure 3C*). Furthermore, SPP1 was significantly upregulated in M2-polarized macrophages (*Figure 3D*). Knockdown of SPP1 in M2 macrophages resulted in decreased ARG1 expression and increased TNFα expression (*Figure 3E*). Flow cytometry analysis of M1/M2 markers demonstrated that knockdown of SPP1 in M2 macrophages led to a decrease in the proportion of CD68⁺CD163⁺ cells and an increase in the proportion of CD68⁺CD86⁺ cells (*Figure 3F*). Collectively, these results indicate that the expression level of SPP1 plays a crucial role in regulating macrophage polarization plasticity.

SPP1 in M2 macrophages promotes the progression of PCa

To confirm the role of SPP1 in M2 macrophages in promoting PCa metastasis, we collected conditioned media from M0, M1, and M2 macrophages with knocked-down SPP1 and co-cultured them with PC3 cells. Our results showed that the conditioned media from M2 macrophages significantly promoted the migration of PC3 cells compared to those from M0 macrophages. However, the migration

Transl Androl Urol 2024;13(7):1239-1255 | https://dx.doi.org/10.21037/tau-24-127
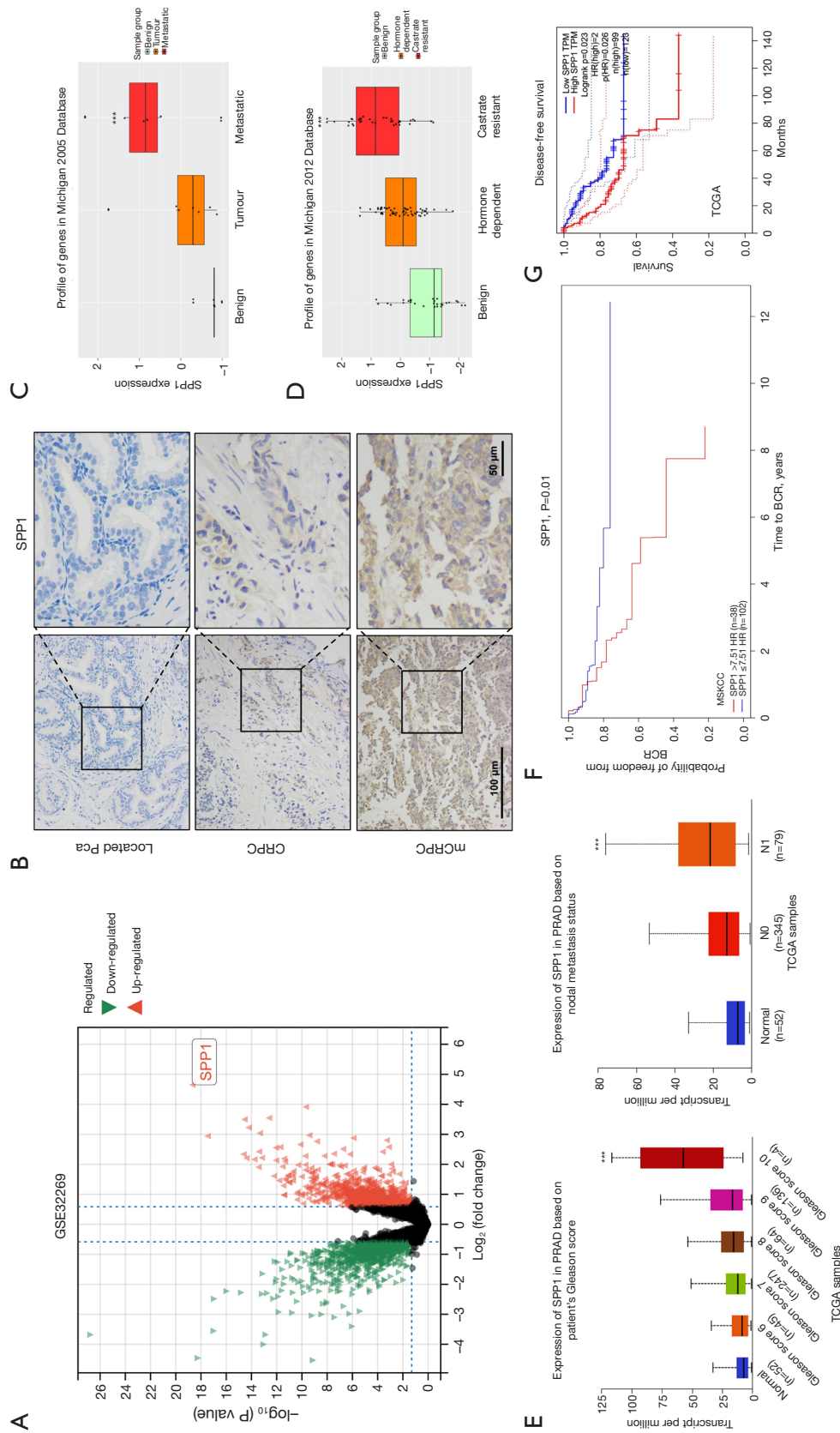
Figure 1 Upregulation of SPP1 is positively correlated with the progression of prostate cancer. (A) Volcano plot of the differentially expressed genes in transcriptome sequencing between 21 cases of located PCa tumor tissues and 29 cases of mCRPC tumor tissues in the GSE32269 dataset. (B) Representative images of SPP1 staining in tissue samples from localized prostate cancer, CRPC, and mCRPC (n=5:5:5; IHC staining). (C,D) Profile of genes in Michigan 2005 and 2012 PCa database shows the expression level of SPP1 among the benign prostate, located prostate tumor, hormone-dependent, and metastatic PCa groups. (E) Analysis of the correlation between the expression of SPP1 and the Gleason score as well as clinical TNM staging in patients with PCa in the TCGA-PRAD database. (F,G) Analysis of the relationship between the expression of SPP1 and the survival period of patients with prostate cancer in the MSKCC and TCGA databases, respectively. ***, P<0.001. SPP1, secreted phosphoprotein 1; PCa, prostate cancer; CRPC, castration-resistant prostate cancer; mCRPC, metastatic CRPC; PRAD, prostate adenocarcinoma; TCGA, The Cancer Genome Atlas; TNM, tumor-node-metastasis; MSKCC, Memorial Sloan Kettering Cancer Center; BCR, biochemical recurrence; TPM, transcripts per million; HR, hazard ratio; IHC, immunohistochemical.
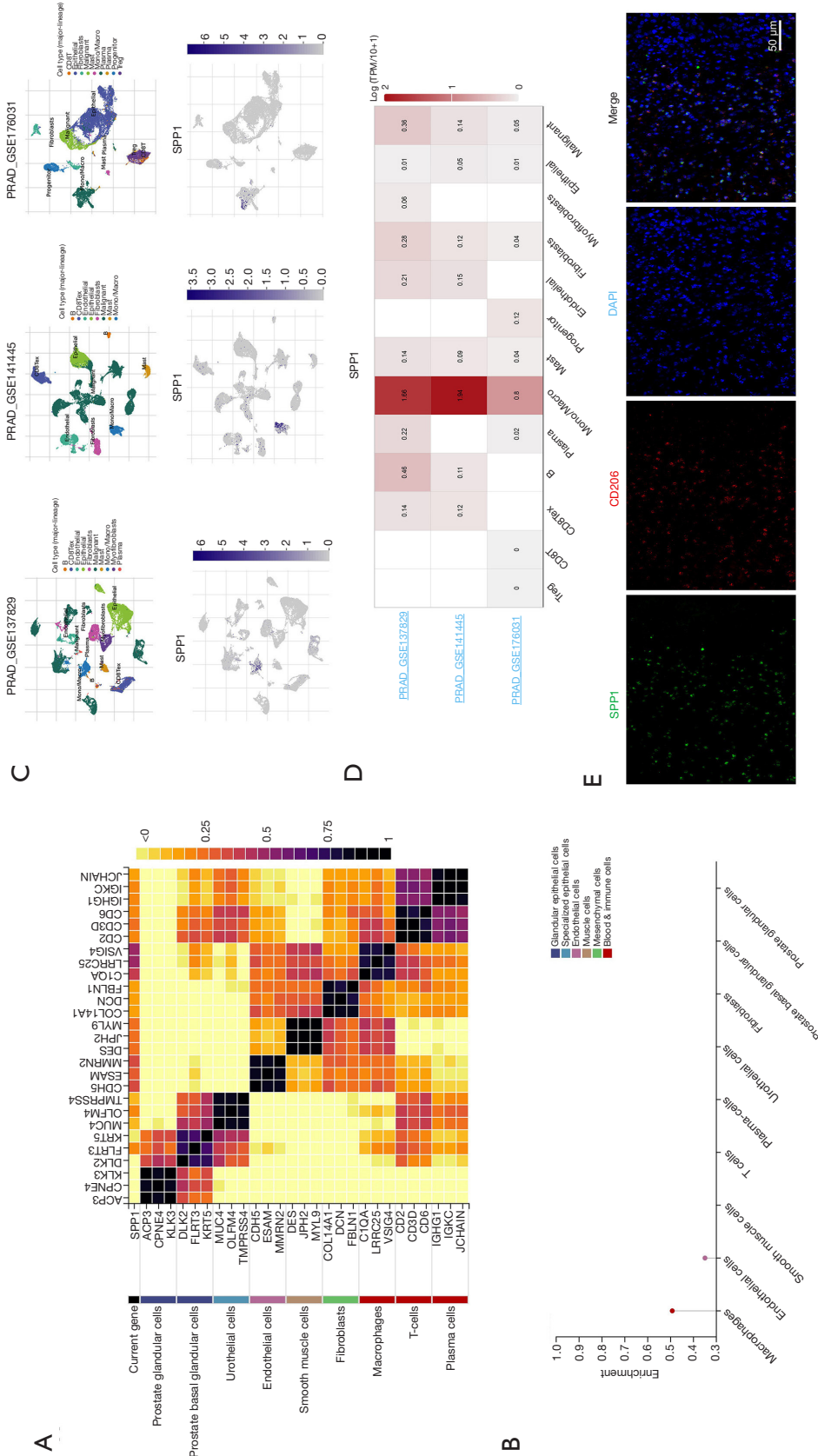
Figure 2 Localization of SPP1 in both prostate and prostate cancer tissues. (A) The correlation between cell type markers and SPP1 in prostate tissue is displayed on heatmaps in the HPA database. (B) Quantitative results of (A). (C) Analysis of the expression levels of SPP1 in different cell types in PCa-related datasets GSE137829, GSE141445, and GSE176031 in the TISHC2 single-cell database. (D) The digital quantization result of (C). (E) Representative merged immunofluorescence image of the co-localization of SPP1 (green) with CD206 (red) positive cells in the samples from mCRPC patient's tumor tissue in (B). The nucleus is stained with DAPI (blue). SPP1, secreted phosphoprotein 1; PRAD, prostate adenocarcinoma; TPM, transcripts per million; Treg, regulatory T; HPA, Human Protein Atlas; PCa, prostate cancer; TISHC2, tumor immune single-cell hub 2; mCRPC, metastatic castration-resistant prostate cancer; DAPI, 4',6-diamidino-2-phenylindole.
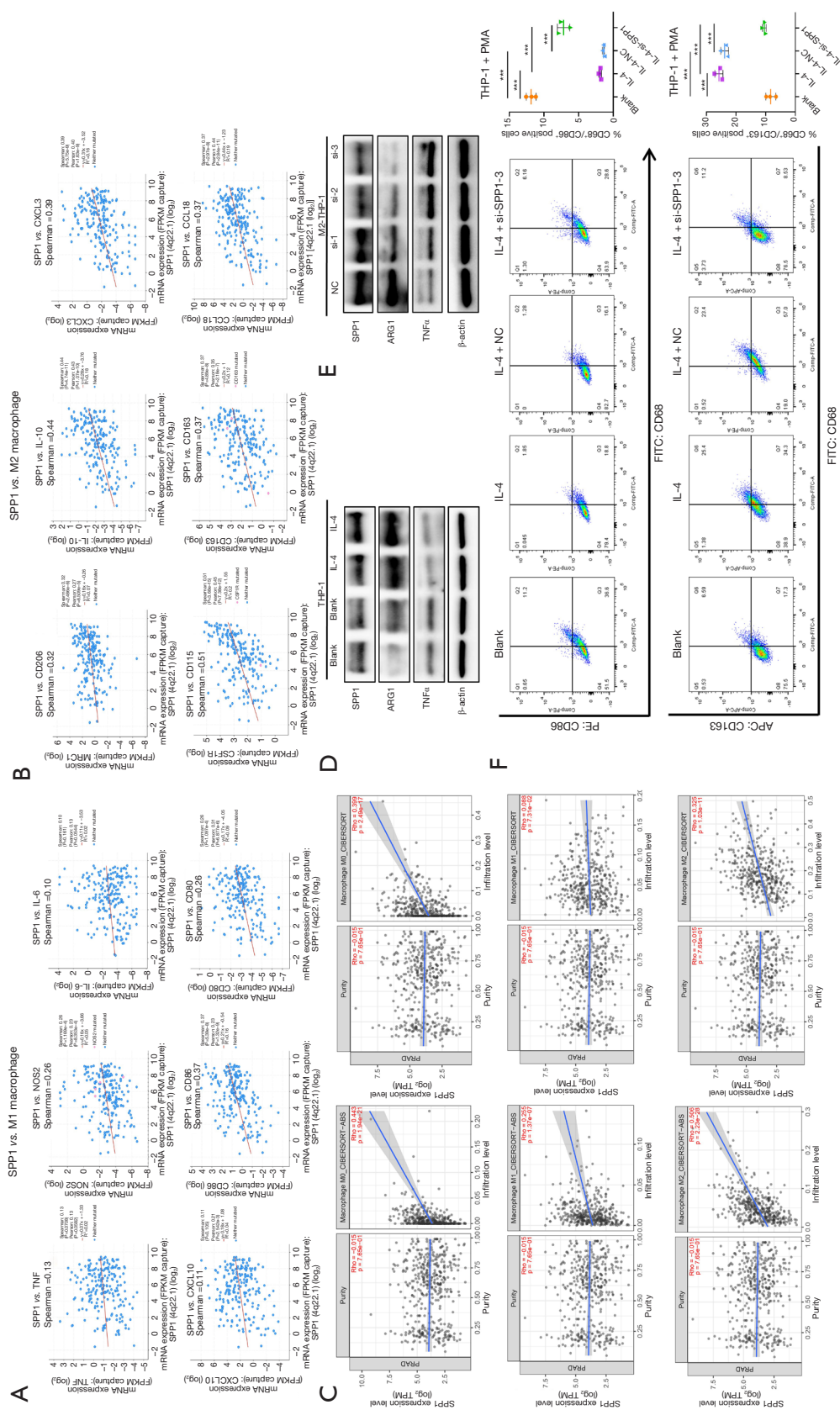
Figure 3 The expression of SPP1 in macrophages is associated with polarization transformation. (A,B) Analyzing the correlation between SPP1 and macrophage M1 and M2-related biomarkers in the SU2C-mCRPC dataset. (C) Correlation between the expression of SPP1 and the infiltration degree of M0/M1/M2 macrophages in prostate cancer analyzed with CIBERSORT and CIBERSORT-ABS methods in the TIMER2.0 database. (D) Western blot experiment to verify successful induction of M2 macrophages. (E) Validation of knockdown effects of three siRNA sequences of SPP1 and expression of macrophage polarization markers in M2 macrophages. (F) Flow cytometry was used to detect the induction of M2 macrophages by THP-1 and expression of CD68^{+}, CD86^{+}, and CD163^{+} cells in M2 macrophages after knocking down SPP1. The quantified results are displayed on the right side. All data are the mean ± standard deviation, an ANOVA was used in (F). ***, P<0.001. FPKM, fragments per kilobase of transcript per million fragments mapped; SPP1, secreted phosphoprotein 1; TPM, transcripts per million; NC, negative control; si, small interfering; PE, phycoerythrin; FITC, fluorescein isothiocyanate; APC, allophycocyanin; PMA, phorbol-12-myristate-13-acetate; ANOVA, analysis of variance.

capability of PC3 cells was significantly weakened when cultured in conditioned media from M2 macrophages with knocked-down SPP1 (*Figure 4A*). Similarly, Transwell assays demonstrated a substantial increase in the invasive and migratory capabilities of PC3 cells when exposed to conditioned media from M2 macrophages. However, this effect was attenuated when SPP1 was knocked down (*Figure 4B*). These findings demonstrate that the expression of SPP1 in M2 macrophages significantly influences the invasion and migration of PC3 cells.

To validate the function of SPP1 *in vivo*, we implanted luciferase-labeled RM1 mouse PCa cells into the orthotopic prostate of C57BL mice. The experimental group was treated with the SPP1 inhibitor TAA at a dose of 100 mg/kg/day. At 3 days after implantation, similar fluorescence values were observed between the control group and the inhibitor group in the orthotopic prostate. However, on day 33, it was found that the fluorescence intensity in the inhibitor group was significantly reduced (*Figure 4C,4D*). By measuring the volume and weight of isolated prostate tumors, we found that the inhibitor-treated group exhibited a significant reduction in the size and weight of PCa tumors compared to the control group (*Figure 4E-4G*). IHC staining results showed a significant downregulation of SPP1 expression and a marked decrease in the number of M2 macrophages in the inhibitor-treated group, resulting in significant inhibition of tumor progression (*Figure 4H*). These findings provide further evidence that SPP1 in M2 macrophages mediates the progression of PCa.

Inhibiting the expression of SPP1 in macrophages significantly reduces tumor metastasis and bone destruction

In the mouse model of orthotopic PCa, the SPP1 inhibitor group exhibited significant suppression of tumor proliferation. To assess orthotopic metastasis of PCa, *in vivo* imaging tests were conducted 33 days after orthotopic implantation of PCa cells in mice. In the control group, a portion of mice showed orthotopic metastasis of PCa, specifically liver and spleen metastasis (*Figure 5A*). In contrast, no metastatic lesions were observed in any locations other than the prostate site in the inhibitor group (*Figure 5B*). Furthermore, the expression of the epithelial marker CDH1 was upregulated, while the mesenchymal markers CDH2, SNAIL, and vimentin were significantly downregulated in the CMC-TAA treat group (*Figure 5C*).

To evaluate tibial tumor metastasis, a mouse tibial

tumor model was established, and tibial fluorescence was detected on days 3 and 33. The live imaging results demonstrated that tumor proliferation in the inhibitor-treated mice was significantly inhibited, with some tumors no longer exhibiting fluorescence (*Figure 5D*). Subsequent histopathological examination, including H&E staining, TRAP staining, and IHC staining, revealed a noteworthy reduction in bone trabecular destruction in the inhibitor group. Moreover, the number of osteoclasts and CD206+ macrophages was remarkably decreased compared to the control group (*Figure 5E*). The TRAP cells (indicated by red arrows) and CD206+ cells (indicated by red arrows) were statistically analyzed and presented (*Figure 5F*). These results collectively demonstrate that inhibiting SPP1 expression in M2 macrophages can significantly impede PCa metastasis.

SPP1 regulates the expression of MMP9 in M2 macrophages through the activation of the PI3K/AKT signaling pathway

To investigate the specific mechanisms underlying the role of SPP1 in PCa progression, we analyzed SPP1-associated genes in two PCa single-cell datasets, namely GSE143791 and GSE137829. Among these genes, *MMP9* exhibited the highest correlation with SPP1 (*Figure 6A*). Further analysis of the SU2C-mCRPC dataset revealed that *MMP9* ranked second in terms of its correlation with SPP1, with a Spearman correlation coefficient of 0.79 (*Figure 6B*). Moreover, a significant correlation between SPP1 and MMP9 was confirmed in the TCGA-PRAD database (*Figure 6C*). Interestingly, the PCa single-cell dataset indicated that MMP9 is primarily expressed in macrophages (*Figure 6D*).

To validate the impact of *MMP9* on PCa progression, we conducted scratch assays and Transwell experiments using conditioned media from MMP9-knockdown M2 macrophages. The results confirmed that the invasion and migration of PC3 cells were significantly inhibited (*Figure 6E,6F*). This suggests that SPP1 in M2 macrophages regulates the expression of MMP9, thereby promoting PCa progression.

To further explore the relationship between SPP1 and *MMP9*, we analyzed the genes associated with *MMP9* in the GSE32269 dataset and performed GSEA. The results revealed a close association between *MMP9* and the PI3K/AKT signaling pathway (*Figure 6G*). Given that SPP1 is a phosphorylated protein and both SPP1 and *MMP9* are
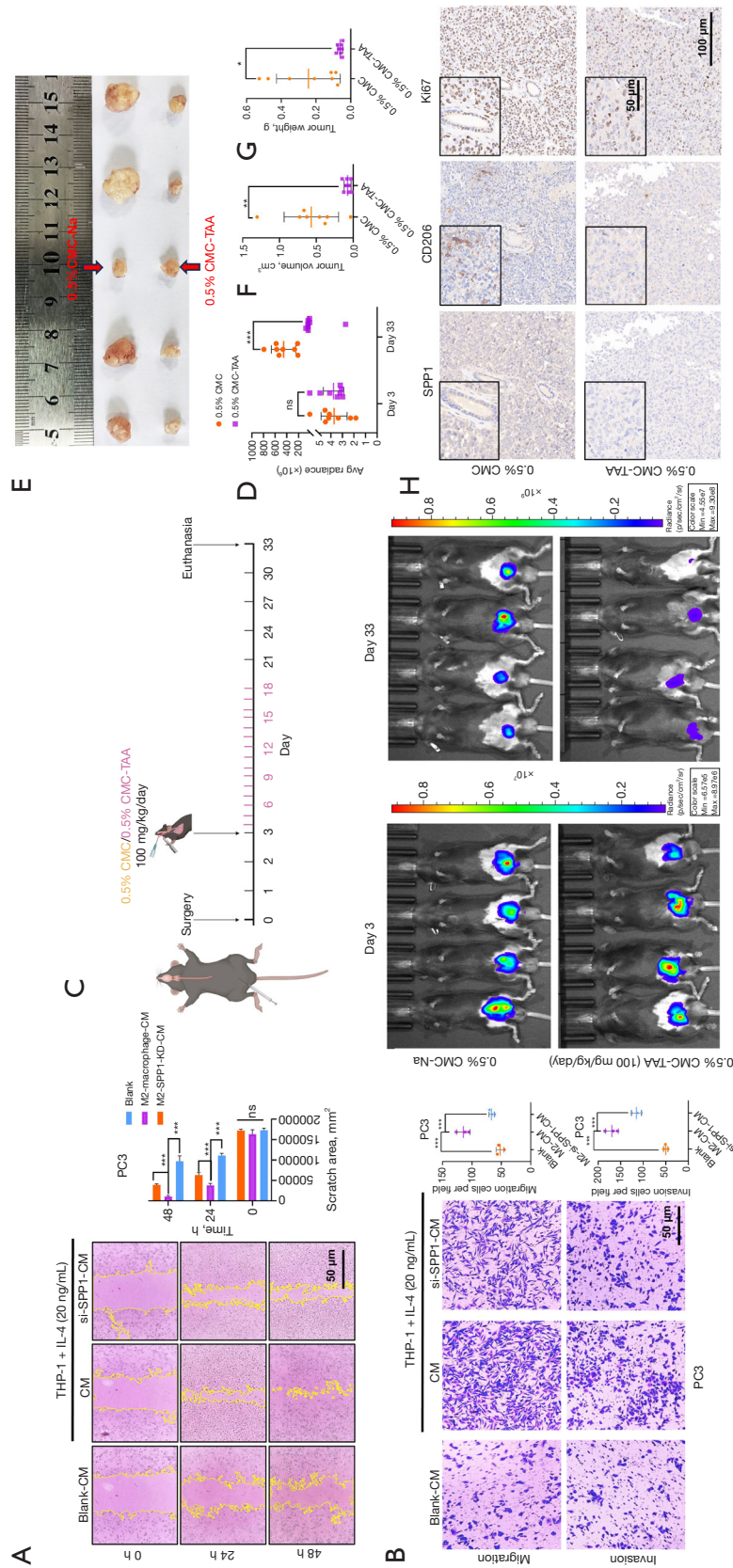
Figure 4 SPP1+ M2 macrophages promote the progression of prostate cancer. (A) Cell scratch experiments were conducted to verify the effect of M0/M2 macrophages and M2 macrophages knocking down SPP1 conditioned medium on the migration ability of PC3 cells. Right is the quantified result of the scratch area. (B) Representative images show the effects of M0/M2 and M2 knockdown of SPP1 conditioned medium on the invasion and migration ability of PC3 cells. The quantitative results of transmembrane cells were stained with crystal violet and shown on the right, with each result repeated 3 times and 3 randomly selected fields of view. (C) Representative BLI images of mice after orthotopic implantation of luciferase-labeled RM1 cells on day 3 and day 33 (n=4:4). (D) Prostate fluorescence of surviving mice on day 33. (E) The volume of prostate tumors *in vitro* in the inhibitor and control group mice was measured using the formula $V = L \times W^2/2$, where L represents the long diameter and W represents the short diameter. (F,G) The volume and mass of isolated prostate tumors separately. (H) Representative image of the immunohistochemical staining of SPP1, CD206, and Ki67 in two groups of mice tumor tissues. All data are the mean ± standard deviation. ANOVA was used in (B), two-tailed unpaired Student's *t*-test was used in (A,E,F,G). *, P<0.05; **, P<0.01; ***, P<0.001. ns, no significant; CM, conditioned medium; SPP1, secreted phosphoprotein 1; KD, knockdown; CMC, carboxymethyl cellulose; TAA, thioacetamide; Ave, average; si, small interfering; BLI, bioluminescence imaging; ANOVA, analysis of variance.
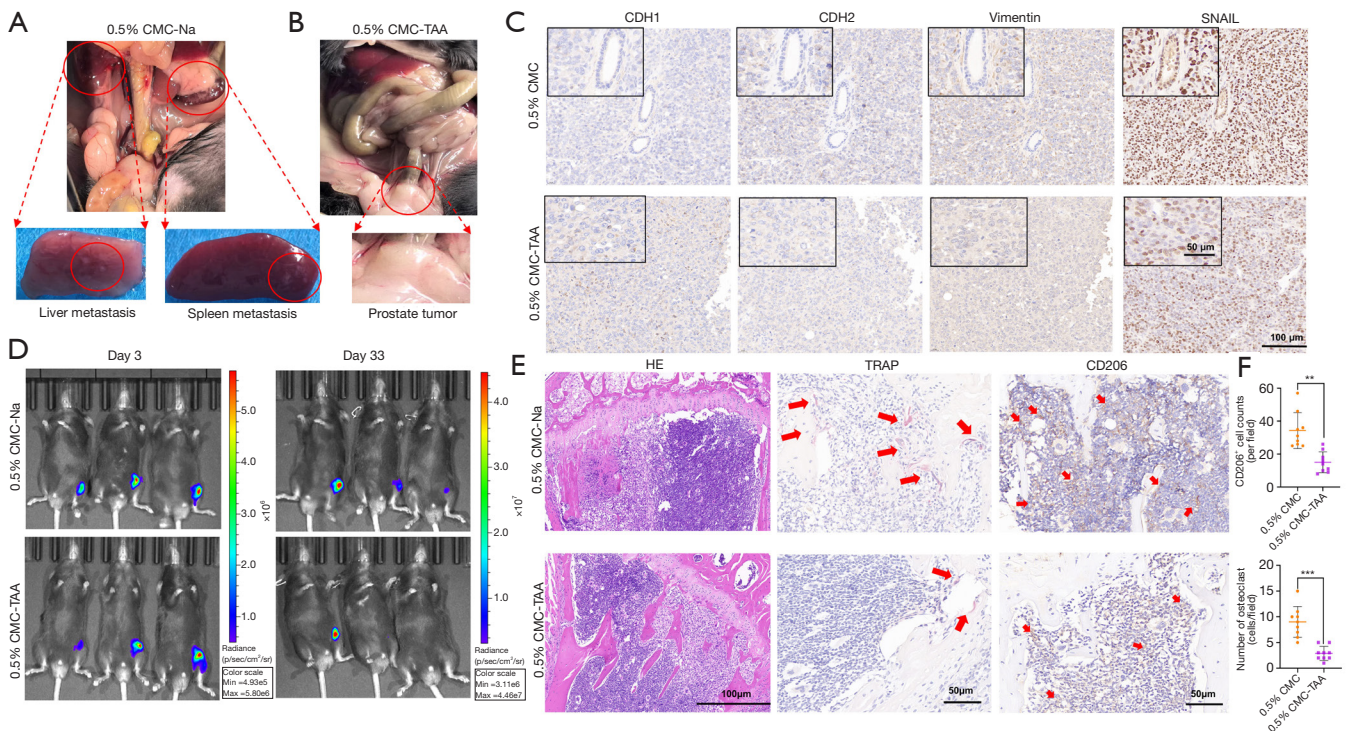
Figure 5 The expression of SPP1 in macrophages participates in tumor metastasis and bone destruction. (A,B) Representative living images of tumor metastasis and non-metastasis on day 33 after surgery. Prostate tumors and metastasis tumors in mouse abdominal organs were represented by red circles (n=2:2). (C) Immunohistochemical detection of EMT-related indicators CDH1, CDH2, vimentin, and SNAIL expression. (D) Representative BLI images of fluorescence value of left lower limb tibia in control group and inhibitor group mice (n=3:3). (E) Representative images of H&E, TRAP staining, and immunohistochemical staining were used to detect bone trabecular destruction, osteoclast formation, and CD206 positive macrophage count, the red arrow represents staining positive cells. (F) Quantify the number of osteoclasts and M2 macrophages. All data are the mean ± standard deviation and analyzed by Two-tailed unpaired Student's t-test. **, P<0.01; ***, P<0.001. CMC, carboxymethyl cellulose; TAA, thioacetamide; SPP1, secreted phosphoprotein 1; EMT, epithelial-mesenchymal transition; H&E, hematoxylin and eosin; TRAP, tartrate-resistant acid phosphatase.

expressed in macrophages in PCa, we found that knocking down SPP1 in M2 macrophages led to reduced MMP9 expression and inhibition of the PI3K/AKT signaling pathway (*Figure 6H*). Additionally, by adding recombinant SPP1 to SPP1-knockdown cells, we observed upregulated MMP9 expression and restored phosphorylated AKT protein expression (*Figure 6I*). These findings suggest that SPP1 regulates MMP9 expression through the activation of the PI3K/AKT signaling pathway.

MMP9 facilitates the EMT of PC3 cells by promoting the processing of TGFβ through the activation of the SMAD2/3 pathway

Previous research has shown that the matrix metalloproteinase

(MMP) family can cleave the latency-associated peptide (LAP) of TGF-β, leading to its activation and subsequent release of TGF-β ligands (20). Intriguingly, KEGG pathway enrichment analysis of differentially expressed genes co-expressed with SPP1 and MMP9 in the SU2C-mCRPC database revealed an enrichment of the TGFβ signaling pathway in both cases (*Figure 7A,7B*). In the mCRPC database, correlation analysis between the three molecules of the TGFβ family (TGFβ1, TGFβ2, TGFβ3) revealed that both SPP1 and MMP9 had the highest correlation with TGFβ1 (*Figure 7C*). Further analysis of the mCRPC database confirmed the ability of TGFβ1 to promote EMT by revealing the correlation between TGFβ1 and EMT-related molecules (CDH1, CDH2, vimentin, SNAIL) (*Figure 7D*). We verified that conditioned medium from
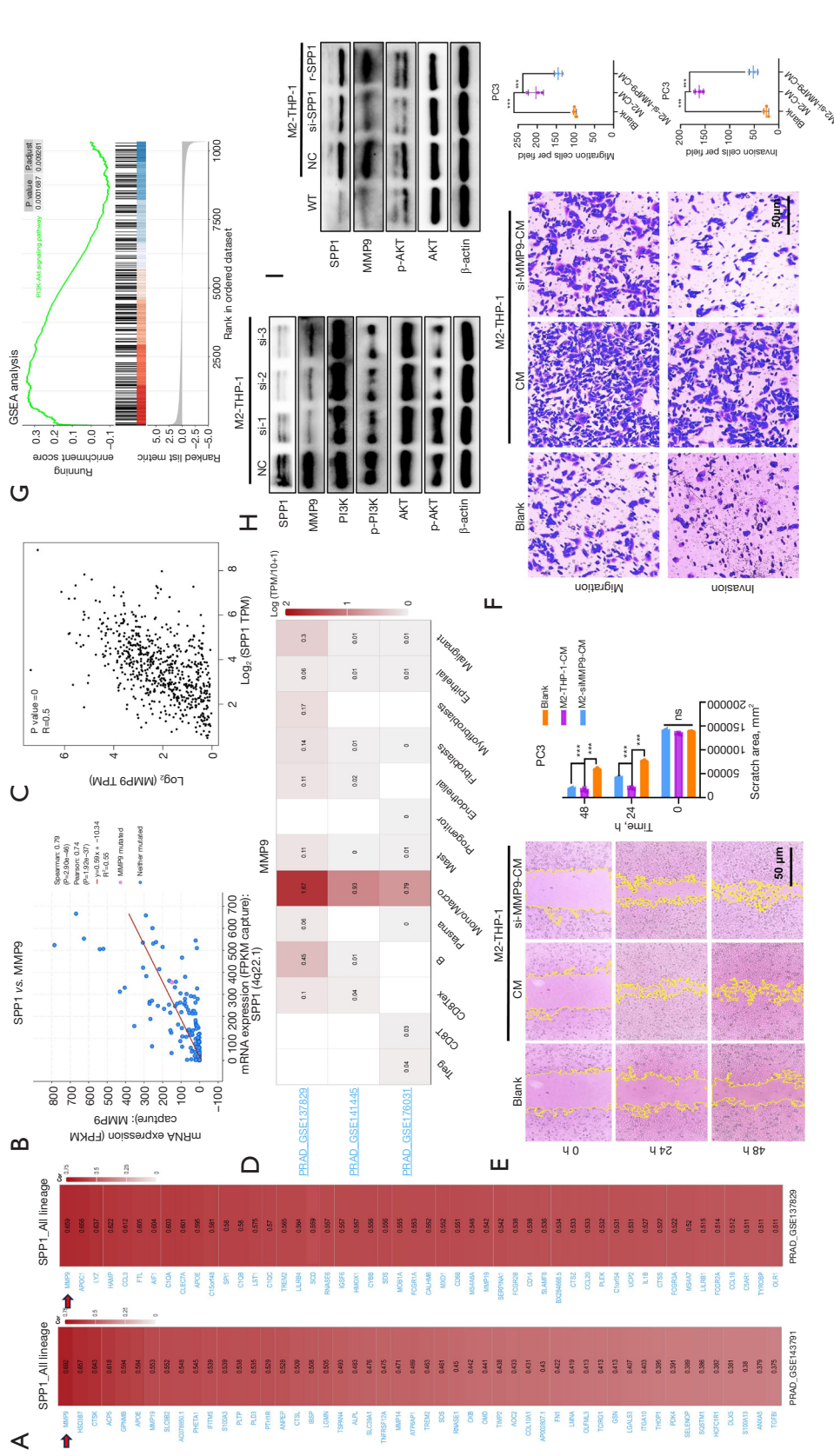
Figure 6 SPP1 promotes the expression of MMP9 progression by activating the PI3K/AKT signaling pathway in M2 macrophages. (A) Analyze the genes related to SPP1 in datasets GSE143791 and GSE137829 in the TISCH2 database. (B) Detecting the correlation between SPP1 and MMP9 in the SU2C-mCRPC cohort. (C) Analyzing the correlation between SPP1 and MMP9 in the TCGA-PRAD database. (D) Expression of MMP9 in different cell types in the TISCH2 prostate cancer single-cell dataset. (E) Cell scratch experiments verified the effect of M0/M2 macrophages and M2 macrophages knocking down MMP9 CM on the migration ability of PC3 cells. Right is the quantified result of the scratch area. (F) Representative images show the effects of M0/M2 and M2 knockdown of SPP1 CM on the invasion and migration ability of PC3. The quantitative results of transmembrane cells were stained with crystal violet and shown on the right. (G) GSEA of MMP9-related genes in GSE32269. (H) Detection of MMP9 and PI3K/AKT signaling pathway expression after knocking down SPP1 in M2 macrophages using western blot assay. (I) Western blot detected the expression of MMP9 and AKT pathway after using r-SPP1 protein in M2 macrophage SPP1-KD. All data are the mean ± standard deviation, ANOVA was used in (F), two-tailed unpaired Student's t-test was used in (E). ***, $P<0.001$. SPP1, secreted phosphoprotein 1; PRAD, prostate adenocarcinoma; FPKM, fragments per kilobase of transcript per million fragments mapped; MMP9, matrix metallopeptidase 9; TPM, transcripts per million; Treg, regulatory T; CM, conditioned medium; ns, no significant; GSEA, gene set enrichment analysis; NC, negative control; WT, wild type; si, small interfering; r-SPP1, recombinant SPP1; TISCH2, tumor immune single-cell hub 2; mCRPC, metastatic castration-resistant prostate cancer; The Cancer Genome Atlas; KD, knockdown; ANOVA, analysis of variance.

1252

Chen et al. SPP1⁺ M2 macrophages promotes the progression of CRPC
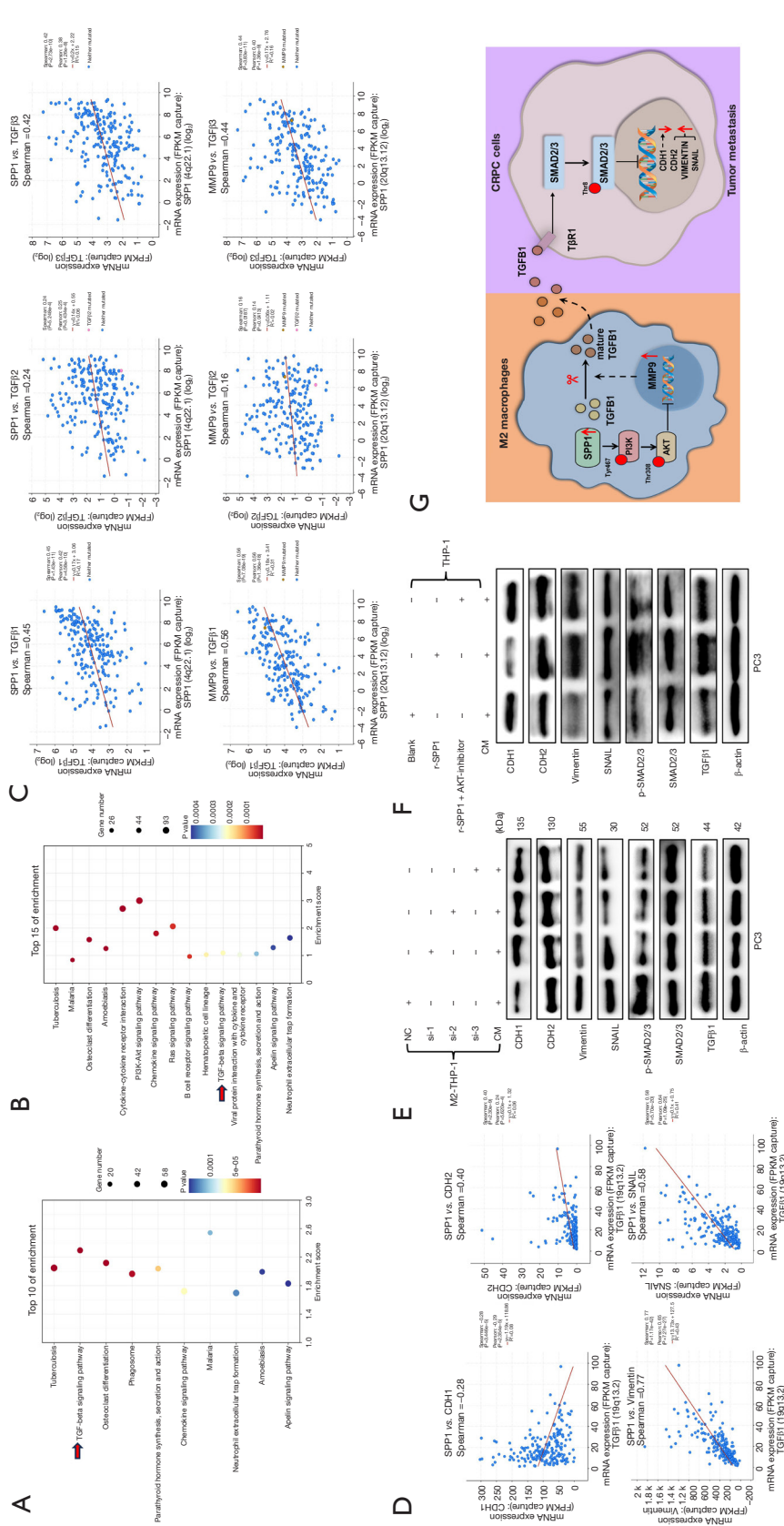
Figure 7 MMP9 activates the TGFβ/SMAD signaling pathway and promotes EMT transformation in PC3 cells. (A,B) KEGG signaling pathway enrichment analysis of differentially expressed genes SPP1 and MMP9 co-expressed in SU2C-mCRPC cohort. The red arrow indicates co-enriched TGFβ signaling pathway. (C) SU2C-mCRPC cohort was used to analyze the correlation between SPP1, MMP9, TGFβ1, TGFβ2, and TGFβ3. (D) Analyze the correlation between TGFβ1 and EMT indicators (CDH1, CDH2, vimentin, and SNAIL) in the SU2C mCRPC cohort. (E) The impact of CM from M2 macrophages with knocked-down SPP1 on the activation of the TGFβ signaling pathway and the ability to induce EMT in PC3 cells was assessed using western blot experiments. (F) THP-1 cells were cultured in separate conditions using r-SPP1 and r-SPP1 with an AKT inhibitor-supplemented medium to assess their effects on PC3 cell EMT and the SMAD2/3 signaling pathway. (G) The schematic diagram of this study. TNF, tumor necrosis factor; SPP1, secreted phosphoprotein 1; FPKM, fragments per kilobase of transcript per million fragments mapped; NC, negative control; si, small interfering; CM, conditioned medium; r-SPP1, recombinant SPP1; CRPC, castration-resistant prostate cancer; MMP9, matrix metallopeptidase 9; EMT, epithelial–mesenchymal transition; KEGG, Kyoto Encyclopedia of Genes and Genomes; mCRPC, metastatic CRPC.

SPP1-knockdown M2 macrophages led to downregulation of phosphorylated SMAD2/3 and stromal markers CDH2, vimentin, and SNAIL, whereas the epithelial marker CDH1 was upregulated in PC3 cells (*Figure* 7E). Subsequently, we added recombinant SPP1 and recombinant SPP1 protein along with an AKT phosphorylation inhibitor to THP-1 cells and co-cultured them with PC3 cells. The results showed that the SMAD2/3 signaling pathway was activated in the group treated with recombinant SPP1 protein, whereas it was deactivated in the group treated with the AKT inhibitor (*Figure* 7F). The schematic diagram of this study is as follows: Overexpression of SPP1 in M2 macrophages activates the PI3K/AKT signaling pathway, promoting the expression of MMP9. Subsequently, MMP9 cleaves TGFβ1, leading to its maturation and increased secretion, which binds to receptors on PC3 cells, activating downstream SMAD2/3 signaling. This ultimately regulates the expression of EMT markers in the nucleus, promoting the metastasis of PCa (*Figure* 7G). These experiments confirmed that the activation of the TGFβ1/SMAD2/3 signaling pathway mediated by MMP9 is a potential mechanism for promoting the progression of PCa.

Discussion

In our study, we innovatively propose that high expression of SPP1 in M2 macrophages promotes the malignant progression of castration-resistant PCa. Mechanistically, we found that the upregulation of SPP1 in M2 macrophages increased the expression of MMP9 through activation of the PI3K/AKT signaling pathway. The increased secretion of MMP9 in M2 macrophages facilitated the TGFβ signaling pathway in PCa cells, thereby enhancing their invasive, migratory, and EMT transformation capabilities. Finally, we applied an SPP1 inhibitor in an orthotopic PCa metastasis model and observed a significant inhibition of tumor progression, along with a noticeable reduction in the recruitment of M2 macrophages in the TME.

PCa exhibits significant heterogeneity compared to other tumors, as the cold reactivity of immunotherapy distinguishes it significantly from other tumors (8). The TME is the main driving force for tumor occurrence and development, and its complex cellular components and intercellular communication are important factors that constitute this network. According to relevant research, TME plays an important role in tumor progression, metastasis, immune suppression, and drug resistance (21,22). Macrophages are representative cell types in the

TME (10), and in recent years, SPP1 macrophages have been found to promote the progression of various tumors. In colon cancer, small cell lung cancer, and liver cancer, blocking the expression of SPP1 in macrophages has been found to increase sensitivity to immune therapy, thereby inhibiting tumor progression (23,24). However, it has not yet been confirmed whether SPP1 macrophages play a role in promoting castration-resistant PCa progression. Previous studies on the mechanisms of CRPC progression have primarily focused on SPP1+ cancer-associated fibroblast (CAF) cells, suggesting their high recruitment in the TME and close association with PCa progression (25,26). Nevertheless, our analysis of PCa single-cell data and mCRPC datasets revealed that M2 macrophages constitute the highest proportion in the metastatic microenvironment of CRPC. Additionally, there are currently related studies confirming the ability of M2 macrophages to promote CRPC progression (3,27). Notably, the expression of SPP1 in macrophages is also an indicator for evaluating macrophage polarization (14). When macrophages have high expression of SPP1, they polarize towards M2, which has also been confirmed in our experiment. There has been speculation regarding whether SPP1 macrophages promote the progression of CRPC. In the experiments we designed, we obtained verification that SPP1+ macrophages significantly enhance the invasion and migration of CPRC cells. Moreover, in *in vivo* experiments, the application of an SPP1 inhibitor effectively inhibited the progression of PCa and reduces the presence of M2 macrophages in the TME.

Interestingly, analysis of SPP1-related genes in PCa single-cell datasets and the SU2C-mCRPC cohort revealed that SPP1 is most significantly correlated with MMP9. Moreover, the PCa single-cell database showed that MMP9 is only highly expressed in macrophages, suggesting a potential regulatory relationship between SPP1 and MMP9 in M2 macrophages. Although previous research has confirmed that SPP1 can promote MMP9 expression in fibroblasts by activating the Akt signaling pathway (20), this regulatory mechanism has not been reported in PCa. Therefore, we confirmed in M2 macrophages that SPP1 regulates MMP9 expression through the PI3K/AKT signaling pathway and affects the malignant phenotype of PCa cells. MMP9, a member of the MMP family, has the function of cleaving LAP to activate TGF-β (20), which is consistent with the results of pathway enrichment and suggests that in M2 macrophages, increased MMP9 expression can activate the function of TGFβ1, leading to increased synthesis and secretion of mature TGFβ1.

Upon binding to PCa cell receptors, the classic Smad2/3 signaling pathway is activated, regulating the expression of EMT-related molecules, and ultimately promoting PCa metastasis.

Conclusions

We have proposed for the first time that high expression of SPP1 in M2 macrophages is a key factor in the progression of CRPC. Through in-depth mechanistic analysis, we have confirmed the involvement of the SPP1-PI3K/AKT-MMP9 signaling axis. Furthermore, our further research has uncovered the MMP9-TGFβ1-Smad2/3 signaling axis. Connecting these signaling pathways provides a preliminary explanation for the potential mechanism by which high expression of SPP1 promotes CRPC metastasis in M2 macrophages. Therefore, targeting SPP1 and its associated signaling pathways holds great promise as a therapeutic approach for CRPC. It has significant clinical implications for inhibiting CRPC metastasis and prolonging patient survival.

Acknowledgments

Footnote

Reporting Checklist: The authors have completed the MDAR and ARRIVE reporting checklists. Available at https://tau.amegroups.com/article/view/10.21037/tau-24-127/rc

Data Sharing Statement: Available at https://tau.amegroups.com/article/view/10.21037/tau-24-127/dss

Peer Review File: Available at https://tau.amegroups.com/article/view/10.21037/tau-24-127/prf

Conflicts of Interest: All authors have completed the ICMJE uniform disclosure form (available at https://tau.amegroups.com/article/view/10.21037/tau-24-127/coif). The authors have no conflicts of interest to declare.

Ethical Statement: The authors are accountable for all aspects of the work in ensuring that questions related

to the accuracy or integrity of any part of the work are appropriately investigated and resolved. The study was conducted in accordance with the Declaration of Helsinki (as revised in 2013). All animal studies carried out in this project strictly followed the regulations of the China Nature Conservation Committee and were approved by the Animal Experiment Welfare and Ethics Committee of the Army Medical University (No. AMUWEC20232943), in compliance with institutional guidelines for the care and use of animals.

Open Access Statement: This is an Open Access article distributed in accordance with the Creative Commons Attribution-NonCommercial-NoDerivs 4.0 International License (CC BY-NC-ND 4.0), which permits the non-commercial replication and distribution of the article with the strict proviso that no changes or edits are made and the original work is properly cited (including links to both the formal publication through the relevant DOI and the license). See: https://creativecommons.org/licenses/by-nc-nd/4.0/.

References

1. Siegel RL, Miller KD, Wagle NS, et al. Cancer statistics, 2023. CA Cancer J Clin 2023;73:17-48.
2. Bishr M, Saad F. Overview of the latest treatments for castration-resistant prostate cancer. Nat Rev Urol 2013;10:522-8.
3. Li XF, Selli C, Zhou HL, et al. Macrophages promote anti-androgen resistance in prostate cancer bone disease. J Exp Med 2023;220:e20221007.
4. Chhabra Y, Weeraratna AT. Fibroblasts in cancer: Unity in heterogeneity. Cell 2023;186:1580-609.
5. Caronni N, La Terza F, Vittoria FM, et al. IL-1β(+) macrophages fuel pathogenic inflammation in pancreatic cancer. Nature 2023;623:415-22.
6. Hofbauer LC, Bozec A, Rauner M, et al. Novel approaches to target the microenvironment of bone metastasis. Nat Rev Clin Oncol 2021;18:488-505.
7. Sternberg C, Armstrong A, Pili R, et al. Randomized, Double-Blind, Placebo-Controlled Phase III Study of Tasquinimod in Men With Metastatic Castration-Resistant Prostate Cancer. J Clin Oncol 2016;34:2636-43.
8. Tong D. Selective estrogen receptor modulators contribute to prostate cancer treatment by regulating the tumor immune microenvironment. J Immunother Cancer 2022;10:e002944.
9. Wang D, Cheng C, Chen X, et al. IL-1β Is an Androgen-

Responsive Target in Macrophages for Immunotherapy of Prostate Cancer. Adv Sci (Weinh) 2023;10:e2206889.

10. Komohara Y, Fujiwara Y, Ohnishi K, et al. Tumor-associated macrophages: Potential therapeutic targets for anti-cancer therapy. Adv Drug Deliv Rev 2016;99:180-5.

11. Matsubara E, Yano H, Pan C, et al. The Significance of SPP1 in Lung Cancers and Its Impact as a Marker for Protumor Tumor-Associated Macrophages. Cancers (Basel) 2023;15:2250.

12. Inoue M, Shinohara ML. Intracellular osteopontin (iOPN) and immunity. Immunol Res 2011;49:160-72.

13. Zhao H, Chen Q, Alam A, et al. The role of osteopontin in the progression of solid organ tumour. Cell Death Dis 2018;9:356.

14. Bill R, Wirapati P, Messemaker M, et al. CXCL9:SPP1 macrophage polarity identifies a network of cellular programs that control human cancers. Science 2023;381:515-24.

15. Sathe A, Mason K, Grimes SM, et al. Colorectal Cancer Metastases in the Liver Establish Immunosuppressive Spatial Networking between Tumor-Associated SPP1+ Macrophages and Fibroblasts. Clin Cancer Res 2023;29:244-60.

16. Liu Y, Zhang Q, Xing B, et al. Immune phenotypic linkage between colorectal cancer and liver metastasis. Cancer Cell 2022;40:424-437.e5.

17. Qi J, Sun H, Zhang Y, et al. Single-cell and spatial analysis reveal interaction of FAP(+) fibroblasts and SPP1(+) macrophages in colorectal cancer. Nat Commun 2022;13:1742.

18. Ramadan A, Afifi N, Yassin NZ, et al. Mesalazine, an osteopontin inhibitor: The potential prophylactic and remedial roles in induced liver fibrosis in rats. Chem Biol Interact 2018;289:109-18.

19. Massam-Wu T, Chiu M, Choudhury R, et al. Assembly of fibrillin microfibrils governs extracellular deposition of latent TGF beta. J Cell Sci 2010;123:3006-18.

20. Kramerova I, Kumagai-Cresse C, Ermolova N, et al. Spp1 (osteopontin) promotes TGFβ processing in fibroblasts of dystrophin-deficient muscles through matrix metalloproteinases. Hum Mol Genet 2019;28:3431-42.

21. Wei R, Liu S, Zhang S, et al. Cellular and Extracellular Components in Tumor Microenvironment and Their Application in Early Diagnosis of Cancers. Anal Cell Pathol (Amst) 2020;2020:6283796.

22. Quail DF, Joyce JA. Microenvironmental regulation of tumor progression and metastasis. Nat Med 2013;19:1423-37.

23. Liu Y, Xun Z, Ma K, et al. Identification of a tumour immune barrier in the HCC microenvironment that determines the efficacy of immunotherapy. J Hepatol 2023;78:770-82.

24. Hu J, Zhang L, Xia H, et al. Tumor microenvironment remodeling after neoadjuvant immunotherapy in non-small cell lung cancer revealed by single-cell RNA sequencing. Genome Med 2023;15:14.

25. Wang H, Li N, Liu Q, et al. Antiandrogen treatment induces stromal cell reprogramming to promote castration resistance in prostate cancer. Cancer Cell 2023;41:1345-1362.e9.

26. Li X, Mu P. The Critical Interplay of CAF Plasticity and Resistance in Prostate Cancer. Cancer Res 2023;83:2990-2.

27. Salachan PV, Rasmussen M, Ulhøi BP, et al. Spatial whole transcriptome profiling of primary tumor from patients with metastatic prostate cancer. Int J Cancer 2023;153:2055-67.